Correlative analysis in time and space of turbulent boundary layer over permeable porous slab

Vlassov D.
Universidade Federal do Paraná. DEMEC, Centro Politécnico c/p 19011, Curitiba, PR, Brasil, CEP 81531-990.
vlassov@demec.ufpr.br,

Vargas J.V.C.
Universidade Federal do Paraná. DEMEC, Centro Politécnico c/p 19011, Curitiba, PR, Brasil, CEP 81531-990.
jvargas@demec.ufpr.br,

Sanches R. A. K.
Universidade Federal do Paraná. DEMEC, Centro Politécnico c/p 19011, Curitiba, PR, Brasil, CEP 81531-990.
raks@ufpr.br.

Abstract. *In this paper it is presented the instrumentation, methodology and results of the experimental studies of convection and size of vortex in turbulent boundary layer over a permeable porous slab. Employing hot wire thermo anemometers, a magnetic recorder, a correlator and a time delay block, correlations in time and space were measured between turbulent velocity components. The analysis of the auto-correlation functions has allowed to determinate the propagation velocity of the vortices in the turbulent boundary layer. The results show that the velocity of vortices propagation in the longitudinal direction represents about 80% of the local average velocity. In the perpendicular direction to the slab, the vortices velocity is 2 – 3 times higher than in the longitudinal direction. The vortices that appear in the turbulent nucleus of the boundary layer move to the external border direction with an angle of 60 – 70 degrees. The insufflation in the turbulent boundary layer through the porous wall did not reveal new effects in the turbulence structure, but the insufflation increased considerably the layer thickness (until 120 mm) that allowed a study of the vortices convection in the boundary layer with good accuracy.*

Keywords: *turbulent boundary layer, thermo anemometry, empirical correlations*

1 Introduction

The experimental study of fluid flow near walls in boundary layer theory is still very important to the investigation of effects generated by different actions with the objective of reducing the superficial friction over the wall and of studying heat transfer with it. Nowadays, there is already accumulated deep knowledge about the turbulent boundary layer structure, based on theoretical and experimental research. In parallel, numerical methods have been developed to perform simulations to the direct resolution of the turbulent boundary layer differential equations, based on various semi-empirical hypotheses for the Reynolds turbulent stresses, boundary layer structures and correlation functions.

One of the most effective actions to control the superficial friction and the heat transfer with the wall is the insufflation of a secondary transversal flow in the boundary layer through a porous, permeable or perforated wall. The intensity of insufflation can be determined by an insufflation parameter, like:

$$\overline{V}_W = \frac{V_W}{U_\infty} \tag{1}$$

where: $\overline{V}_W$ - insufflation parameter;
V_W - vertical velocity of insufflation through the porous wall;
U_∞ - horizontal velocity of flow out of the boundary layer.

When the insufflation parameter is small, the semi-empirical theory provides a good approcimation to the experimentally measured data of velocity profiles and other boundary layer characteristics, but with the increase of the insufflation parameter, the agreement between the experimental and theoretical results gets worse and, furthermore, also increases the dispersion of the experimental data from one to another run. In the case of flow over an impermeable wall, the small thickness of the boundary layer and large velocity gradients near the wall complicate or make incorrect the experimental study of turbulence characteristics. Like it was presented in previous works (Vlassov, 2001; Vlassov and Vargas, 2003) the transversal insufflation in boundary layer over plain porous slab generates an abrupt growth of the boundary layer thickness, maintaining its external part preserved.

The birth, growth and dissipation of vortices inside the boundary layer still continue to be a not well explored and not well known part of the turbulent boundary layer theory. However, the knowledge about the vortices size and about

its propagation in the boundary layer can give interesting information and increase the knowledge about the boundary layer structure.

Even in simpler conditions (isothermal boundary layer, plane, without longitudinal pressure gradient, uniform insufflation, etc.) the system of equations of the turbulent boundary layer is not closed. To close the system of equations, various hypotheses are assumed which generally establish correlations between the Reynolds turbulent stresses and the longitudinal medium velocity in the boundary layer. One of the hypotheses, proposed by Glushko (1971), uses a correlation between the turbulent stresses and the vortices size variation through the boundary layer thickness.

The turbulent flow in the boundary layer interacts with the free stream out of the boundary layer. Each of these flows exercises influence over the other. In the case that there's no flow out of the boundary layer, i. e., the fluid is stationary, there is reason to suppose that the coefficients and spatial correlation functions, measured in the boundary layer, are also independent of the time. According to Hinze (1959), in the turbulent boundary layer there are correlations between the turbulent velocity components in two different flow points (bi-dimensional and three-dimensional correlations). These correlations can be used in the analysis of the velocity field variation in the boundary layer. Analyzing the correlations, it is possible to determine places in the boundary layer in which the fluid eddies in various points of the boundary layer are linked to each other, because those places are correlated. The correlation between the turbulent velocity components is characterized by coefficients of spatial correlation.

In the turbulent flow theory, various correlation types are reported. The most important ones are the following double correlations:

i) $R_{u'v'}(0,0,0)$ correlation coefficient in only one point between the turbulent velocity components: longitudinal - u' and vertical - v'. This correlation coefficient is measured from the turbulent intensities in the longitudinal direction - $\sqrt{\overline{u'^2}}$ and vertical direction $\sqrt{\overline{v'^2}}$ in the boundary layer by the equation:

$$R_{u'v'}(0,0,0) = \frac{\overline{u'v'}}{\sqrt{\overline{u'^2}}\sqrt{\overline{v'^2}}} \tag{2}$$

In practice, this equation is used to calculate the Reynolds turbulent stresses.

ii) Spatial Euler correlations are determined between two turbulent velocity components in various points of the boundary layer. For example, the correlation function, $R_{u'u'}(\Delta x,0,0) = f(x)$, determines the variation of the correlation coefficient between two points Δx in the axis *x*, in which the longitudinal components of turbulent velocity u' are measured. Other correlation function, $R_{u'u'}(0,\Delta y,0) = f(y)$, determines the correlation coefficient $R_{u'u'}(0,\Delta y,0)$ between the longitudinal components of the turbulent velocity u' as a function of the distance between two points Δy in the axis *y* of the boundary layer where these components are measured.

These two correlation functions allow the determination of macro (macro-scale) and micro (micro-scale) scales of turbulence in the boundary layer. In other words, the correlation function forms $R_{u'u'}(x,0,0) = f(x)$ and $R_{u'u'}(0,y,0) = f(y)$ allow the determination of the size of macro (large) vortices that are also known as the macro-scale or the integral scale in the boundary layer in the longitudinal direction. The macro-scale in the longitudinal and vertical directions are determined by the equations:

$$L_x = \int_0^\infty R_{u'u'}(x,0,0)dx \text{ and } L_y = \int_0^\infty R_{u'u'}(0,y,0)dy \text{, respectively.} \tag{3}$$

where: L_x - vortex size in the axis *0-x*;

L_y - vortex size in the axis *0-y*.

The process of generation and dissipation of vortices in the boundary layer is continuous. The vortices are born, grow, and achieve their maximum size, and after that, due to the fluid viscosity, a dissipation process occurs. Then, vortices of various sizes from L_x to vortices of micro-scale λ_R remains simultaneously in the boundary layer. The turbulence micro-scale λ_R is the average vortices size of the smallest sizes existing in the boundary layer, through which the energy dissipation happens in the turbulent boundary layer, because there is transformation of kinetic energy in to heat, due to the fluid viscosity.

In order to determine the vortices propagation velocity inside the boundary layer it is used the time correlation coefficient of Lagrange $R(0,0,\Delta\tau)$, where: τ is the time, that is also called autocorrelation coefficient. The autocorrelation function $R(0,0,\Delta\tau) = f(\tau)$ allows the determination of the residence time in the boundary layer of a correlated volume of the fluid beside a point in the boundary layer where it is measured the correlation coefficient.

2. Experimental model, flow parameters and instrumentation

The experimental part of the work was performed in a subsonic aerodynamic tunnel with an Eiffel chamber (Fig. 1). The tunnel was made from wood and the Eiffel chamber made with steel. In the nozzle entrance of this tunnel it was placed a honeycomb, to make the air flow uniformly at the entrance. The area reduction of the nozzle was around 15 times. The test section was made in shape of a regular octagon with the distance between opposite sides of 800 mm and the length of 1750 mm. The air current in the tunnel was created with a 12 blade fan located in the diffuser outlet. The fan, by means of an electromagnetic glove, was connected to an alternate current electric motor. The electromagnetic valve was used to control the fan speed. To avoid the influence of a casual electric tension and temperature variation in the pieces of the actuating mechanism of the fan on the fan speed, it was installed an electronic scheme with a tachometer and a reaction coupling. During the runs, with the aid of this scheme, the fan speed was kept constant, providing a constant value of air flow velocity in the test section.

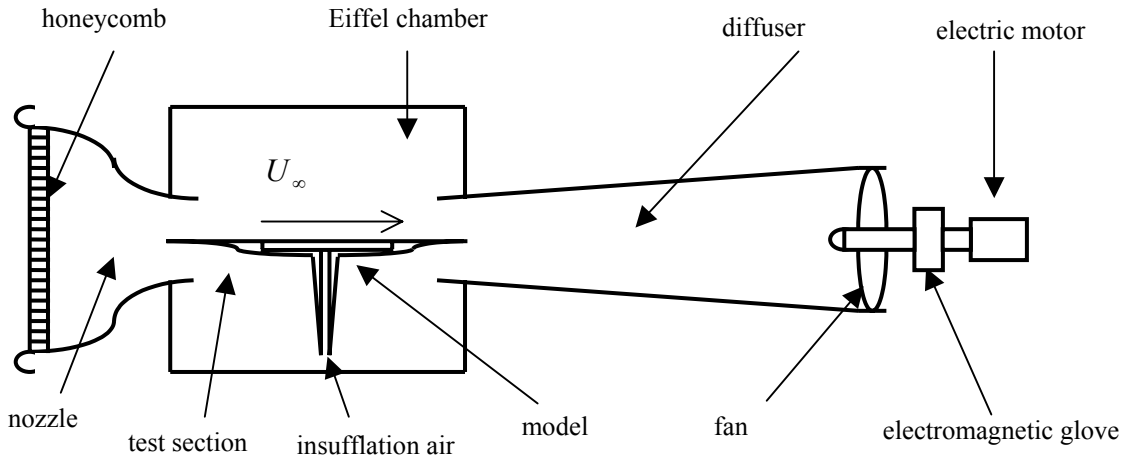

Figure 1 - Aerodynamic tunnel scheme.

The air flow parameters in the tunnel were the following: the air velocity in the tunnel test section was sustained as U_∞=10 m/s (±0,5%); the turbulence ratio of the air current $\varepsilon = \frac{\sqrt{\overline{u'^2}}}{U_\infty} 100\%$ in the test section varied from 0.5% in the nozzle outlet, up to 0.7% in the diffuser entrance (where $\sqrt{\overline{u'^2}}$ - dispersion of the longitudinal velocity turbulent component); the air temperature varied from 18 to 30 ºC, and the longitudinal pressure gradient in the test section was null, $\frac{dp}{dx} = 0$.

The experimental model consisted of a smooth and plain slab, with a total length of 2530 mm and width of 400 mm. The slab was composed by a forward impermeable part with length of 1000 mm, by a permeable porous slab part with length of 1030 mm and by a rear impermeable part with a length of 500 mm. The forward length allowed a developed turbulent boundary layer in the porous initial part, $Re_x = \frac{xU_\infty}{\nu} \approx 6{,}5 \times 10^5$. The rear length was selected to prevent the influence of the flow separation in the rear border of the model on the boundary layer development.

The porous slab was manufactured by hot lamination in vacuum of a stainless steel web bundle (steel grids). The bundle was composed by 20 layers of grids with relatively thick wires, that granted the necessary strength to the porous slab. Over these 20 layers, other 8 layers of thin grids, made from wire with 0.09 mm, with square cells of 0.14 × 0.14 mm. More 10 layers of even thinner grids were added, with diameter of 0.055 mm with cells of 0.071 × 0.071 mm. The use of the last thin grid layers in the bundle (that after the lamination compose the external working surface of the porous slab) allowed to have the minim surface roughness and small pores sizes. The slab dimensions after finishing were: length - 1030 mm, width - 399 mm and thickness-7.75 mm. The medium porosity *P* of the slab porous material was 11.8%. The material porosity was calculated by the equation:

$$P = \frac{\rho_c - \rho_p}{\rho_c} 100\%, \tag{4}$$

where: ρ_c - stainless steel density;

ρ_p - porous material density.

The microscopic analysis showed that the average value of the pores diameter in the surface was 15 μm. The porous slab was welded over a box with impermeable walls with a height of 80 mm. Inside the box, under the porous slab, was installed a system of uniform distribution of the insufflation air.

The uniformity of air insufflation to the porous slab surface was verified using a micro-flow meter, made based on a thermo-anemometer. The variation of the insufflation velocity in the entire porous slab surface stayed in a range of ±10% and in the center of the slab, where the measures of the boundary layer parameter were performed, it was in the range of ±5%. During the experiment, the insufflation air velocity V_W was varied discretely, admitting the values: V_W = 0.0; 0.05; 0.1; 0.142; 0.18; 0.212; 0.243 m/s. The conditions were isothermal, because both the air in the tunnel and the insufflation air had the same temperature.

The measurements of the boundary layer parameters were made using an experimental equipment made by the Danish manufacturer DISA. The electronic blocks diagram of the measurement system is shown in Fig. 2. The components were: 1 – thermo anemometers 55D01; 2 – linearizers 55D10; 3 – filters 55D25; 4 – addition and subtraction blocks to obtain the longitudinal (u') and vertical (v') turbulent velocity components; 5 – voltmeter for alternate current 55D35; 6 – electromagnetic recorder with 20 channels of frequency modulation "Uran" to continuously record the measured parameters and the post processed parameters; 7 – correlation coefficient meter 55A06; 8 – delay line to measure the autocorrelation coefficients.

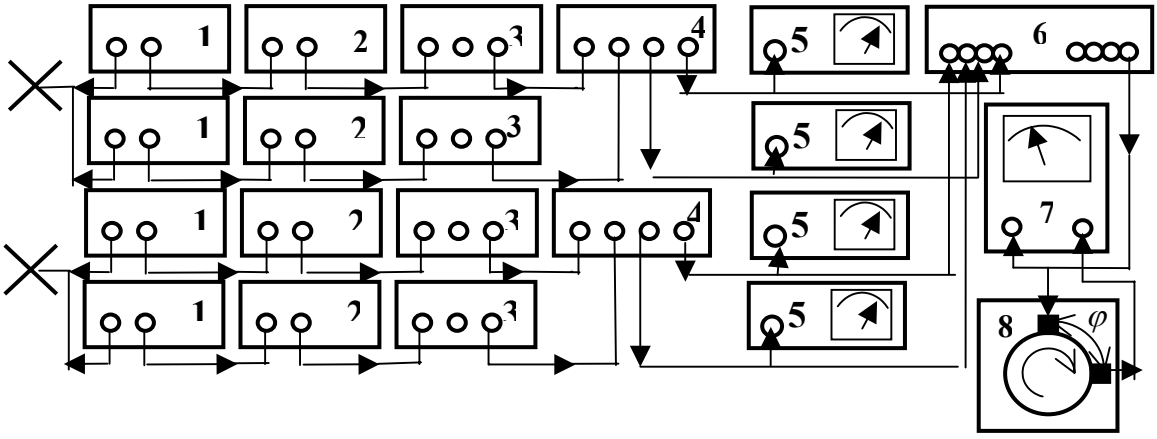

Figure - 2 Electronic block diagram of the experimental apparatus.

In order to measure the turbulent velocity components, transducers of two hot wires "in X" of model X55A38 were utilized, with the wires length of 1 mm, diameter of 0.005 mm. The hot wires were placed with 45º in X from the transducer axis. The wires were made with wolfram, with a slim external coating of platinum to prevent oxidation.

To accomplish the displacement of X-transducers through the boundary layer, it was utilized a spatial coordinator with remote control. The coordinator stayed out of the airflow in the tunnel. Inside the flow stayed only the supports to the X-transducers. The coordinator had three degrees of freedom: horizontal displacement of the transducers along the slab through the axis *x*; vertical displacement along the axis *y*; and angular displacement around the axis *y*. The coordinator had the linear precision along the axis *x* of ± 0.5 mm, along the axis *y* of ± 0.01 mm and angular precision of ± 0.5º. The initial distance of the thermo anemometer transducer from the slab wall was measured with an optical cathetometer with the precision of 0.001 mm and focal distance of 650 mm.

3. Methodology

In order to measure the correlation coefficients, two X-transducers were placed in the boundary layer, following the scheme shown in the Fig. 3. The separation and measurement of the turbulent velocity components u' and v' were made employing the known methodology of two Thermo-anemometers 1 (Fig. 2) to each of the wires of the X-transducer. The electric signals of the thermo anemometers were linearized in the linearizers 2. At the exit of the Filters 3, the electric signals are proportional to $u'+v'$ and $u'-v'$. Next, the electric signals are driven to the summing and subtraction Block 4. In the Blocks 4, the signals proportional to $u'+v'$ and $u'-v'$ were added, receiving a value proportional to u' and the second was subtracted from the first receiving a value proportional to v'. From the addition and subtraction blocks 4, result the signals of u' and v' from two X-transducers. These signals were measured with the Voltmeter for alternate current 5. The signals of the two X-transducers were recorded in the electromagnetic Recorder 6 or a pair of them was driven to the correlator 7 to measure correlation coefficient.

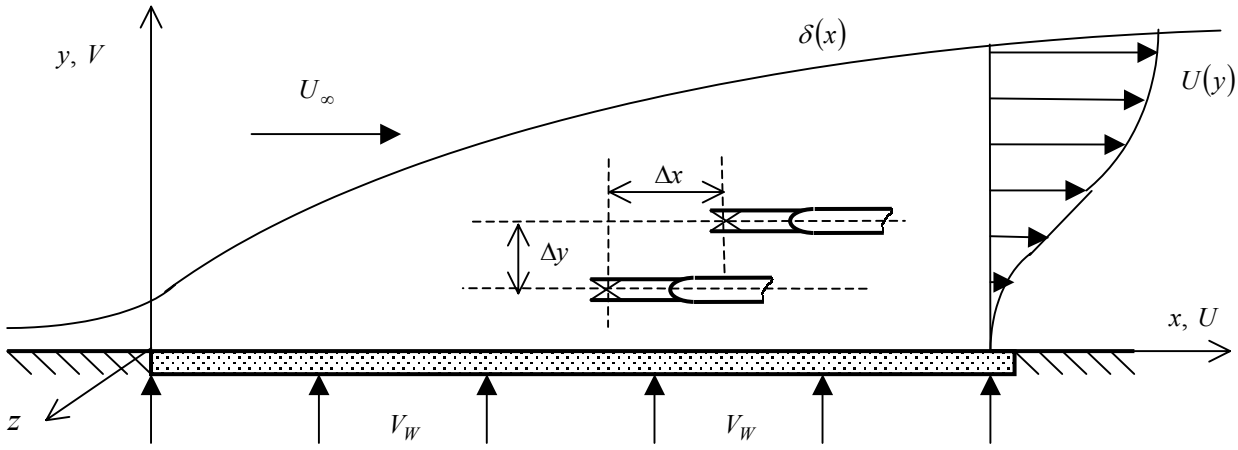

Figure 3 Flow scheme and disposition of the X – transducers in the boundary layer.

Before measuring the Euler spatial correlation coefficients $R_{u'u'}(x,0,0) = f(x)$ and $R_{u'u'}(0,y,0) = f(y)$, the X-transducers were placed in a point in the boundary layer. It is obvious that the distance between the wires crossing point of the two X-transducers was a distance in the transversal direction to the flow (along the axis *z*, Fig. 3). The X-transducers can never be positioned at the same point in the boundary layer, therefore the values of $R_{u'u'}(x,0,0)=1.0$ and $R_{u'u'}(0,y,0)=1.0$ cannot be measured. Then, keeping one of the transducers fixed, the other was displaced along the axis *x* or along the axis *y*, changing (increasing) discretely the values of Δx or Δy, respectively.

To measure the Lagrange correlation coefficient in time $R(0,0,\Delta\tau)$ the signal recorded in the electromagnetic recorder was driven to the delay line. The signal delay line has a routing disc with an electromagnetic layer on its face and systems of frequency modulation and demodulation. While measuring the correlation coefficient in time, the disc maintained the angular speed of rotation constant, $\omega = Const$ [rad/s]. The delay line had two heads. One of them, the recorder head, is fixed and the other is the signal reproduction head that is mobile along a circumference with an angle $\Delta\varphi$ [rad] with respect to the fixed recorder head (see Fig 2). The delay time $\Delta\tau$ is determined by $\Delta\tau = \frac{\varphi}{\omega}$ [s]. The process of measuring the correlation coefficient in time was the following: the electric signal proportional to u' (coming directly from the X-transducer or from the electromagnetic recorder) was driven simultaneously to the correlator and to the delay line. In the delay line, the signal was frequency modulated and recorded in the routing disc. Passing to the reproduction head, the signal was read, demodulated and driven to the correlator, in which the correlation coefficient was measured in time. To increase the delay time of $\Delta\tau$, the angle was increased of $\Delta\varphi$ or the angular speed reduced of ω (maintaining its value constant during the measurement).

4. Experimental results.

In Fig. 4, it is shown an autocorrelation function $R_{u'u'}(0,0,\Delta\tau) = f(\Delta\tau)$ and also several curves of spatial correlation functions in time $R_{u'u'}(\Delta x,0,\Delta\tau) = f(\Delta x,\Delta\tau)$. The fixed transducer was in the boundary layer in the distance of *x*= 700 mm from the porous slab leading edge. The insufflation parameter was $\overline{V_W} = 0.005$. The boundary layer thickness in this section was $\delta = y_{\overline{U}=0,99} =$ 45 mm, *y* = 12 mm ($\overline{U} = 0.667$). When the spatial correlation coefficients were measured in time, one of the transducers stayed fixed and the other was discretely displaced along the axis *x*, maintaining *y* = *const*.

The autocorrelation function $R_{u'u'}(0,0,\Delta\tau) = f(\Delta\tau)$ shows a maximum value of 1 when $\Delta\tau = 0$. With the delay time of ~8 ms, the correlation coefficient becomes null.

The spatial correlation functions in time, $R_{u'u'}(\Delta x,0,\Delta\tau) = f(\Delta x,\Delta\tau)$ allow the determination of the velocity of vortices propagation in the boundary layer. To determine the vortices velocity in the boundary layer, correlation coefficients were measured between the signals of the mobile and fixed transducers at a distance Δx between them. The fixed transducer signal passed through the delay line. The delay time was varied in a range such that the optimum value of the delay time was found, which corresponds to the maximum correlation coefficient value $R_{u'u'}(\Delta x,0,\Delta\tau)$. For example, for the distance between transducers Δx_{opt}=30,0 mm (Fig. 4) the optimum value of the delay time is

~5 ms. The average velocity of vortices propagation in the boundary layer in the longitudinal direction ϑ_x and vertical direction ϑ_y are calculated by:

$$\vartheta_x = \frac{\Delta x}{\Delta \tau_{ot}} \text{ e } \vartheta_y = \frac{\Delta y}{\Delta \tau_{ot}} \tag{5}$$

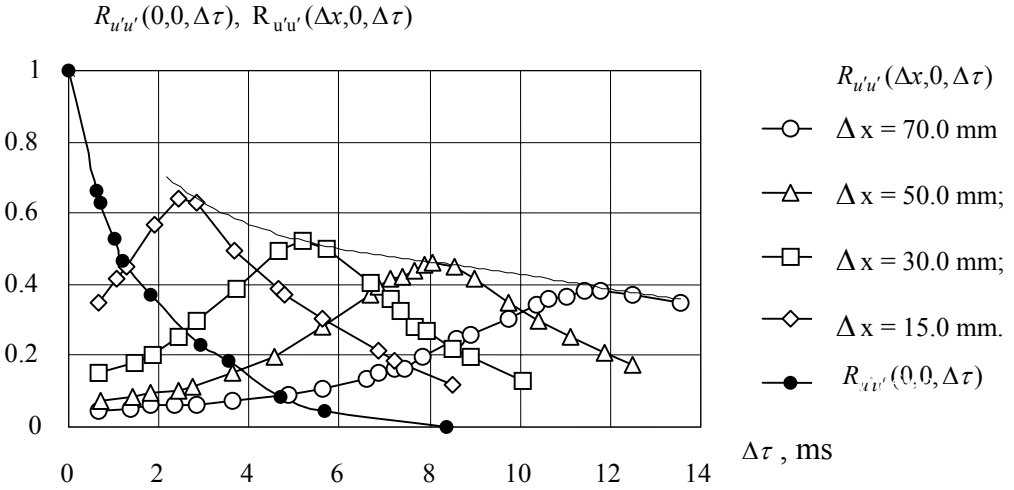

Figure 4 - Auto-correlation function $R_{u'u'}(0,0,\Delta\tau)$ and correlation curves $R_{u'u'}(\Delta x,0,\Delta\tau)$ to several distances between the X –transducers.

In Figure 5 it is shown the longitudinal nondimensional velocity $\overline{\vartheta_x} = \frac{\vartheta_x}{U}$ of vortices propagation as a function of the insufflation parameter $\overline{V_W}$.

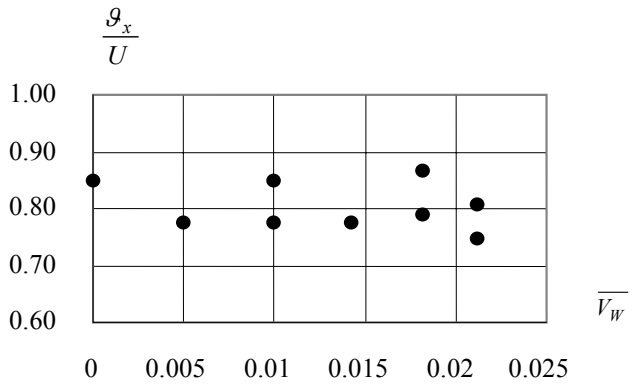

Figure 5 - Nondimensional longitudinal velocity of vortices propagation as a function of the insufflation parameter.

For all insufflation parameters $\overline{V_W}$, the fixed transducer was placed in the boundary layer in a point were $U = \frac{2}{3}U_\infty$. This value of U was chosen because at this point of the turbulent boundary layer, independently of the insufflation parameter, the turbulent stresses and the intensity of the turbulent velocity components achieve maximum values (Vlassov and Vargas, 2003). As it is shown in the Fig. 5, the velocity of vortices propagation does not depend on the insufflation parameter and it is approximately 80% of the local longitudinal velocity. The vortices in the horizontal direction are slightly delayed with respect to the local velocity.

In the vertical direction the result is different. In Figure 6 it is presented the vertical nondimensional velocity $\overline{\vartheta_y} = \frac{\vartheta_y}{U}$ of vortices propagation as a function of the insufflation parameter.

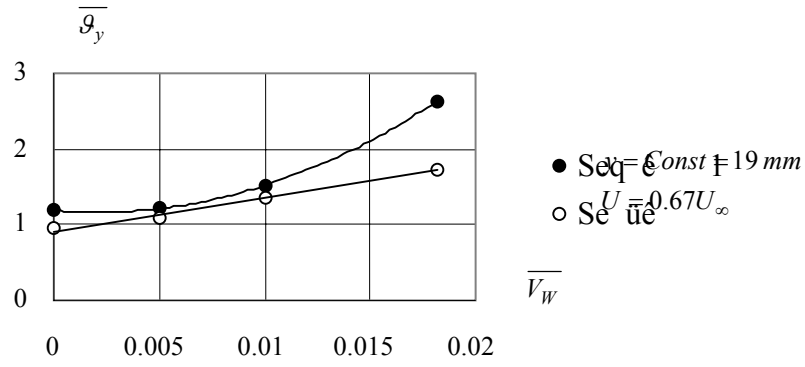

Figure 6 - Vertical nondimensional velocity of vortices propagation versus the insufflation parameter.

The measurement of the vertical velocity of vortices propagation in the boundary layer was performed using two methods. The first is like in the longitudinal component case when the fixed transducer was placed in the boundary layer in a place that the longitudinal average velocity is equal to $U = 0.67U_\infty$. And the second was used when, independently of the insufflation parameter, the distance of the fixed transducer was maintained constant and equal to $y = Const = 19\ mm$. The measurement results in Fig. 6 show that the vertical component of the velocity of vortices propagation in the boundary layer depend on the insufflation parameter $\overline{V_W}$. Without the insufflation, when $\overline{V_W} = 0.0$, the longitudinal and vertical vortices components are almost equal, because $\overline{\vartheta_x} \approx \overline{\vartheta_y}$. With an increase of $\overline{V_W}$ the vertical component of the vortices velocity grows and the longitudinal component continues to be insensitive to the insufflation. It is interesting to compare the numerical values. For the insufflation parameter of $\overline{V_W} = 0.018$, the vertical component of the average velocity at the wall is only $V_W = 0.18$ m/s, but in the case in witch the fixed transducer was placed in the point $U = 0.67U_\infty$, the components of the vortices velocity were $\vartheta_x = 5.6$ m/s and $\vartheta_y = 12$ m/s. In the case when $y = Const = 19$ mm, for the same value $\overline{V_W} = 0.018$, the average longitudinal velocity was of 3.3 m/s and the vertical component of the vortices velocity was $\vartheta_y = 8.9$ m/s. The comparison of the data in Figs. 5 and 6 shows that the vertical components of the vortices velocity are 2 to 3 times higher than the longitudinal component. The vortices propagate to the external side of the turbulent boundary layer with an angle of 60º to 70º. The vortex born near the wall is quickly accelerated and dissipated on the external side of the boundary layer.

In Figure 7 it is shown the spatial correlation function $R_{u'u'}(0,\Delta y,0) = f(y)$. Measurements were made in section $x = 700$ mm from the porous slab leading edge, with the insufflation parameter $\overline{V_W} = 0.0212$.

The measurement of the correlation coefficients shown in Fig. 7 shows that the correlation between the turbulent velocity components exists in almost the entire boundary layer thickness δ (in this case $\delta = 90$ mm). It is known that in the case of turbulent boundary layer, the external border is not stable. In the external side of the turbulent boundary layer, the flow has intermittent characteristics, because the free stream flow out of the boundary layer (that has low turbulence intensity) is alternating with the turbulent flow generated by the vortices release to the outside of the boundary layer. The intermittency phenomenon disappears in a distance δ_{int} from the wall, that is higher than the boundary layer thickness δ (in this case $\delta_{\text{int}} = 99$ mm).

When the mobile transducer is still inside of the intermittency zone ($y < \delta_{\text{int}}$) all correlation functions are almost identical. When the mobile transducer goes out of the intermittency zone, the correlation coefficient changes to a low negative value.

Other peculiarity of the correlation curves is that they decrease abruptly under low values of $\pm\Delta y$, when the distance between the fixed transducer and the mobile one is still small. This phenomenon can be explained by the presence of high frequency turbulence components.

Starting from the correlation functions, substituted into Eq. (3), macro turbulence scales were calculated in the boundary layer, L_x and L_y along the axis x and y, respectively. The results are shown in Figs. 8 and 9 in the nondimensional forms $L_x/\delta = f\left(y/\delta\right)$ and $L_y/\delta = f\left(y/\delta\right)$. The computed numerical values of the macro scales can be obtained from Table 1, that shows values of the boundary layer thickness in section $x = 700$ mm from the porous slab leading edge (in which the measurements were performed) for insufflation parameters used in the experiment.

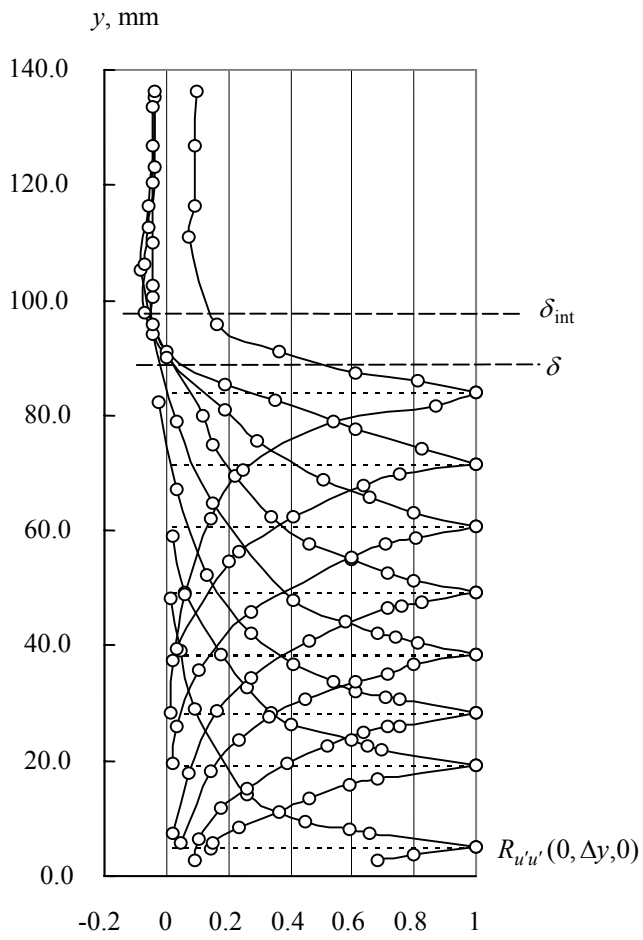

Figure 7 - Correlation functions in the vertical-to-wall direction

Table 1 - Thickness of the boundary layer as a function of the insufflation parameter in section x = 700 mm

$\overline{V_W}$	0.0	0.005	0.01	0.0142	0.0182	0.0212	0.0243
δ (mm)	39	45	53	62	72	85	99

From what is seen in Figs. 8 and 9, the longitudinal macro scale is almost two times higher than the macro scale along the vertical axis, because the vortices are extended along the boundary layer.

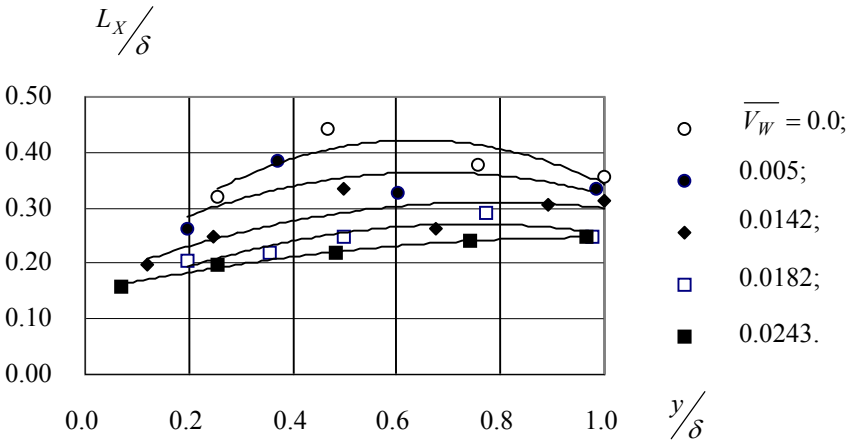

Figure 8 - Longitudinal macro scales versus insufflation parameter for x = 700 mm.

The transversal insufflation to the boundary layer substantially reduces the macro scales either along the axis x, or along the axis y. In the dimensional scale, the vortices length along the axis x varied from ~ 15 mm to ~ 22 mm.

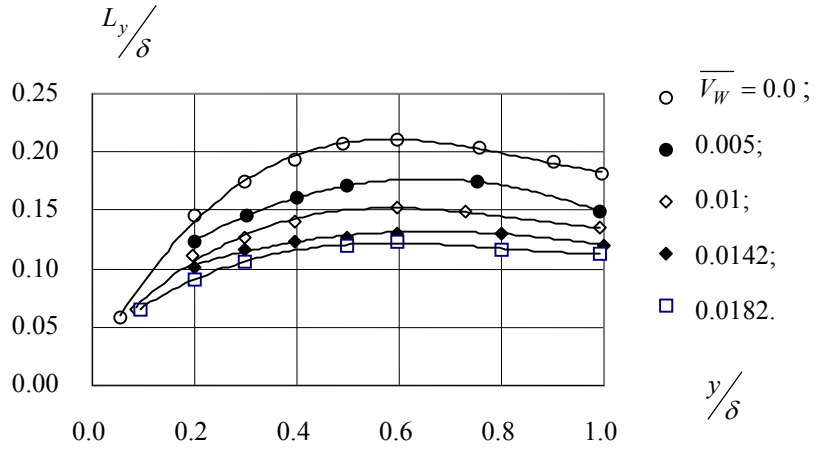

Figure 9 - Vertical macro scales versus insufflation parameter for x = 700 mm.

5. Conclusion

This work presented an experimental study performed in an aerodynamic wind tunnel to determinate empirical correlations for the propagation velocity of the vortices in the turbulent boundary layer on a permeable porous slab. Such correlations are expected to be useful to complete the system of conservation equations for the turbulent boundary layer to be used in numerical simulations of turbulent fluid flow for aero design and optimization purposes both in the industry and academia.

6. References

1. Vlassov D., 2001, “Estrutura de sub-camada viscosa em camada limite turbulenta na placa porosa penetrável”, Proceedings of the 16º Congresso Brasileiro de Engenharia Mecânica. Brazil.
2. Vlassov D., Vargas J. V. C., 2003 “Distribuição de tensões turbulentas em camada limite turbulenta sobre plano poroso permeável”, Proceedings of the 17º Congresso Brasileiro de Engenharia Mecânica. Brazil.
3. Glushko G.S., 1971, “Mecânica de líquidos e gases” N 4.
4. Hinze J. O., 1959, “Turbulence an introduction to its mechanism and theory”, NY, USA.